Near-field SAR for signature and camouflage evaluation in realistic backgrounds

Larsson, Christer; Jersblad, Johan

Published in:
[Host publication title missing]

2011

NEAR-FIELD SAR FOR SIGNATURE AND CAMOUFLAGE EVALUATION IN REALISTIC BACKGROUNDS

Christer Larsson
Saab Dynamics
S-581 88 Linköping
Sweden
and
Department of Electrical and Information Technology
Lund University
P.O. Box 118
S-221 00 Lund
Sweden

Johan Jersblad
Saab Barracuda
S-594 32 Gamleby
Sweden

ABSTRACT

A low cost transportable short range Synthetic Aperture Radar (SAR) measurement system is constructed by placing a linear positioner on the bed of a truck. The radar system is based on a network analyzer and a pair of standard horn antennas. The SAR system gives a resolution of 0.3 m at X-band frequencies and 100 m measurement distance. By using the terrain the objects can be measured at depression angles up to at least 10°. The near field SAR images are processed using back projection algorithms. The system can be used to estimate camouflage efficacy in realistic environments. Flexible software based entirely on open source components is developed for the data processing, presentation and analysis of the SAR images. Results from the evaluation of two generic camouflage nets using reference targets in different backgrounds and SAR images of vehicles are presented.

Keywords: RCS, SAR (Synthetic Aperture Radar), Near-Field, Measurement, Imaging

1 Introduction

Outdoor ranges are commonly used for accurate radar cross section (RCS) measurements of full scale vehicles with or without camouflage. Furthermore, inverse synthetic aperture radar (ISAR) processing is a well established method to obtain high quality radar imagery of the objects [1]. However, the ISAR images do not show the vehicles in the environment where they are supposed to operate. In addition, it is not always feasible to transport the vehicles to the ISAR measurement range. A useful approach in many cases is then to use a SAR system that can be transported to the objects placed in realistic environments.

This paper describes a low cost and transportable ground based SAR system that is used to make accurate measurements on vehicles or other objects in realistic backgrounds. It is constructed by placing a linear postioner with antennas on the bed of an all terrain truck. The approach provides a very stable setup which means that it gives very high reproducibility. The same measurement geometry can therefore be used to record the signature from an object placed in a background environment before and after the addition of a camouflage system such as a camouflage net or a mobile camouflage system. It is then possible to use the two processed images to make a realistic estimate of the camouflage efficacy in this environment.

In comparison to the method presented in this paper, flying SAR needs either two identical vehicles, camouflaged and bare, positioned with high accuracy with respect to each other, or to fly the same route twice over first a camouflaged, and then a bare target. Both methods involving flying SAR are complex and have low accuracy.

Flexible software based entirely on open source components is developed for the data processing, presentation and statistical analysis of the SAR images.

Figure 1. The figure shows the SAR setup. The linear positioner can be seen mounted on the bed of the truck. The elevation gives a SAR look angle of 10°.

We present results from the evaluation of two generic camouflage nets using reference targets in different backgrounds and SAR images of vehicles.

2 Theory

Back projection is used in order to obtain the SAR images. The reflectivity distribution function $\psi(x, y)$ at the image coordinates (x, y) is given by

$$\psi(x,y) = \sum_{\mathrm{m}=1}^{\mathrm{M}} \sum_{\mathrm{n}=1}^{\mathrm{N}} K A(f_{\mathrm{n}}, \mathrm{m}) \mathrm{e}^{(-\mathrm{i}2k_{\mathrm{n}}(r_{\mathrm{m}}(x,y)-r_{\mathrm{m}0}))}, \quad (1)$$

where the sums are performed over the M antenna positions and N frequencies. $A(f_{\mathrm{n}}, \mathrm{m})$ is the measured radar cross section complex valued amplitude for specific transmitted and received polarizations. $A(f_{\mathrm{n}}, \mathrm{m})$ is related to the measured RCS at frequency f_n and antenna position m, $\sigma(f_{\mathrm{n}}, \mathrm{m})$, by $\sigma(f_{\mathrm{n}}, \mathrm{m}) = |A(f_{\mathrm{n}}, \mathrm{m})|^2$. k_{n} is the free space wavenumber at frequency f_{n}, *i.e.*, $k_{\mathrm{n}} = 2\pi f_{\mathrm{n}}/\mathrm{c}_0$ where c_0 is the speed of light. $r_{\mathrm{m}}(x, y)$ is the distance from antenna position m to the image point at (x, y) and $r_{\mathrm{m}0}$ is the distance from antenna position m to the image origin. $K = K_{\mathrm{m}}$ is a normalization constant that corrects for the distance dependence of the signal received from different parts of the imaged region. K_{m} is given by

$$K_{\mathrm{m}} = \left(\frac{1}{\mathrm{MN}}\right)\left(\frac{r_{\mathrm{m}}(x,y)}{r_{\mathrm{m}0}}\right)^2. \quad (2)$$

Equation 1 is basically a discrete version of an expression for $\psi(x, y)$ given in [2].

Geometrically correct images can be obtained by performing the summations in Equation 1 for each image point. A faster way is to calculate a downrange profile for each antenna position from the frequency sweep using a discrete fourier transform (DFT). The downrange profiles are then used for interpolation and summed together coherently to get the combined reflectivity distribution $\psi(x, y)$ at the image coordinates (x, y) [2].

Image gating can be performed to obtain the RCS for parts of an image. An incoherent average over measured frequencies and and angles of the RCS , σ_{G} inside a gate can be obtained by summing the function ψ inside the gate area, G. This can be expressed as

$$\sigma_{\mathrm{G}} = L \sum_{x,y \in \mathrm{G}} |\psi(x,y)|^2, \quad (3)$$

where L is a normalization constant. L can be determined by processing an image for a synthetic isotropic scatterer with σ=1 m^2 and gating it, thereby obtaining the normalization.

Figure 2. The linear positioner mounted on the bed of the truck. The horn antennas, shown in the far end of the rail, are connected with phase-stabilized cables to the PNA network analyzer.

3 Instrumentation

Short range SAR experiments are performed with a Scientific Atlanta linear positioner placed on the bed of a truck as shown in Figures 1 and 2. The target range is 100 – 110 m, which with a 5.4 m linear positioner gives a cross-range resolution of 0.3 m at X-band frequencies. The antennas are

moved along the positioner in 80 equidistant steps for one measurement which takes approximately 5 minutes. The down-range resolution is adjusted to match the cross-range resolution by adjusting the bandwidth to 0.55 GHz with a center frequency of 10 GHz. The bandwidth is swept in 2001 frequency point which gives an ambiguity free range of 545 m which is sufficient for these measurements. The radar system is based on an Agilent E8363B PNA network analyzer without power amplifier and a pair of standard X-band horn antennas oriented for VV polarization measurements.
Coherent calibration is performed using a corner reflector as the calibration target. The calibration is done for all positions of the antennas. This procedure compensates for small misalignments of the linear positioner.
The SAR processing gain is sufficient to provide high quality SAR images limited only by the background clutter.

4 Data Processing

Software is written for processing of the raw data and for the analysis of the SAR images. An open source approach is chosen with two programmatic layers. A top scripting layer is used for graphical user interfaces and operations that are not time critical and a second layer written in Fortran is used for time critical parts of the program. This approach provides excellent performance for this application. The SAR images shown in this paper are processed from calibrated raw data in less than 2 s for each image using a standard PC. Python [3], an advanced object oriented open source language is used for the top level. Some other advantages of Python, besides being open source, are that it is a flexible language that is very easy to learn. It can also be extended with many useful extension modules. Two examples of extension modules that are used in this project are Matplotlib [4] that is used for graphics and PyTables [5] that is used to store and retrieve data from Hierarchical Data Format (HDF) [6] files. This approach also means that the data processing software can be used on different operating systems without rewriting. The software is tested on the Windows and Linux operating systems.

5 Results and discussion

The SAR system is demonstrated by showing the results for two series of measurements. The first series are SAR measurements of a three corner reflector reference target. The three corner reflectors are designed to have a nominal RCS of 20 dBsm, 10 dBsm and 5 dBsm at 10 GHz, respectively. The reference target is camouflaged with generic low and high transmission camouflage nets, using a low-RCS support stand. Photographs of the reference target and the reference target covered by the two different camouflage nets are shown in Figure 3. The corresponding SAR images are processed from calibrated raw data using the procedure outlined in section 2. The resulting Hanning filtered images are shown in Figure 4. The 2.6 m^2 image gates that are used when the RCS is extracted for the 20 dBsm, 10 dBsm and 5 dBsm corner reflectors are denoted 1, 2 and 3. The RCS for the three image gates are determined using Equation 3. This procedure is repeated for the reference target without camouflage and for the reference target camouflaged with the two different nets. The results are presented in Table 1.

Measured config.	**Gate**	**RCS (dBsm)**	**RCS Δ (dB)**
Reference target	1	19.9(-0.3,+0.3)	0.0
	2	10.0(-0.9,+0.8)	0.0
	3	3.9(-2.0,+1.6)	0.0
Low transm.	1	8.4(-0.3,+0.3)	-11.5(-0.6,+0.6)
	2	-3.5(-1.2,+1.0)	-13.5(-2.0,+1.9)
	3	-7.2(-1.9,+1.5)	-11.1(-3.5,+3.5)
High transm.	1	16.9(-0.3,+0.3)	-3.0(-0.6,+0.6)
	2	6.6(-1.0,+0.9)	-3.4(-1.8,+1.8)
	3	1.8(-1.7,+1.5)	-2.1(-3.3,+3.4)

Table 1. The table shows the RCS with estimated limits for the error due to clutter within parenthesis and the RCS reduction with estimated error limits when camouflaged , (RCS Δ), for the three trihedral corner reflectors used in the tests. The measurement configurations correspond to the configurations shown in Figure 3.

The clutter that is present in the images will introduce an error when the RCS values are extracted by image gating. The average clutter RCS level for the image gate size used, 2.6 m^2, is estimated to -10 dBsm by measuring the clutter in a large number of gates outside the target. It is also assumed that the the clutter interfering with the camouflaged reflectors is attenuated the same amount as the 20 m^2 corner reflector RCS is reduced by the camouflage. This means that the background clutter level for the used gate size is estimated to -21.5 dBsm for the low transmission camouflage and to -13 dBsm for the high transmission camouflage. It is then possible to use these clutter levels to estimate error limits for the RCS levels in Table 1. The error limits for the RCS reduction are obtained by adding the error limits of the two terms that are used in the subtraction. It is interesting to note that the determined RCS levels and the RCS reduction of the camouflage for the three different corner reflectors are consistent when the error limits are included.
The difference in the RCS values without and with camouflage net can then be used to determine the efficacy of the camouflage. It is also possible to extract the reflection from the net itself by either removing the reflectors, or positioning the gate where there is no reflector.
The second series of measurements are performed on a T72 tank oriented at 0°, 45°and 90°. Figure 5 shows photographs of the three orientations. The corresponding SAR images are

processed from calibrated raw data and the resulting images are shown in Figure 6. The robustness of these kinds of targets (weight on the order of 50 tons) and the stability of the measurement setup ensures repeatability and offers the possibility of comparative measurements between different camouflage systems. It should be pointed out that it is important that the entire object is stable during the course of one measurements. A loose attachment on the object, flapping in the wind, will cause image artifact that may obscure other details in the SAR image and make analysis more complicated.

6 Conclusions

A low cost transportable X-band SAR system is set up for measurements of objects including camouflage systems in a realistic background. Open source software is used to write the programs that are needed to process, store, analyze and display the data. Furthermore, a method that can be used to evaluate camouflage systems is shown.

Acknowledgements

The financial support by the Swedish Defence Materiel Administration and the technical support from the Swedish Defence Material Administration Test and Evaluation Centre Skövde is gratefully acknowledged. The authors would also like to thank Olof Ahnlund, Hans-Olof Berlin, Martin Norsell, Jonas Rahm and Carl-Gustaf Svensson for their contributions.

7 References

[1] D. L. Mensa, *High resolution radar cross-section imaging*, rev. ed. Boston: Artech House, 1991.

[2] T. Vaupel and T. F. Eibert, "Comparison and application of near-field ISAR imaging techniques for far-field radar cross section determination," *IEEE Trans. Antennas Propagat.*, vol. 54, no. 1, pp. 144–151, 2006.

[3] "Python Programming Language – Official Website," `http://www.python.org`.

[4] "Matplotlib website," `http://matplotlib.sourceforge.net`.

[5] "PyTables home page," `http://www.pytables.org`.

[6] "HDF5 home page," `http://www.hdfgroup.org/HDF5/`.

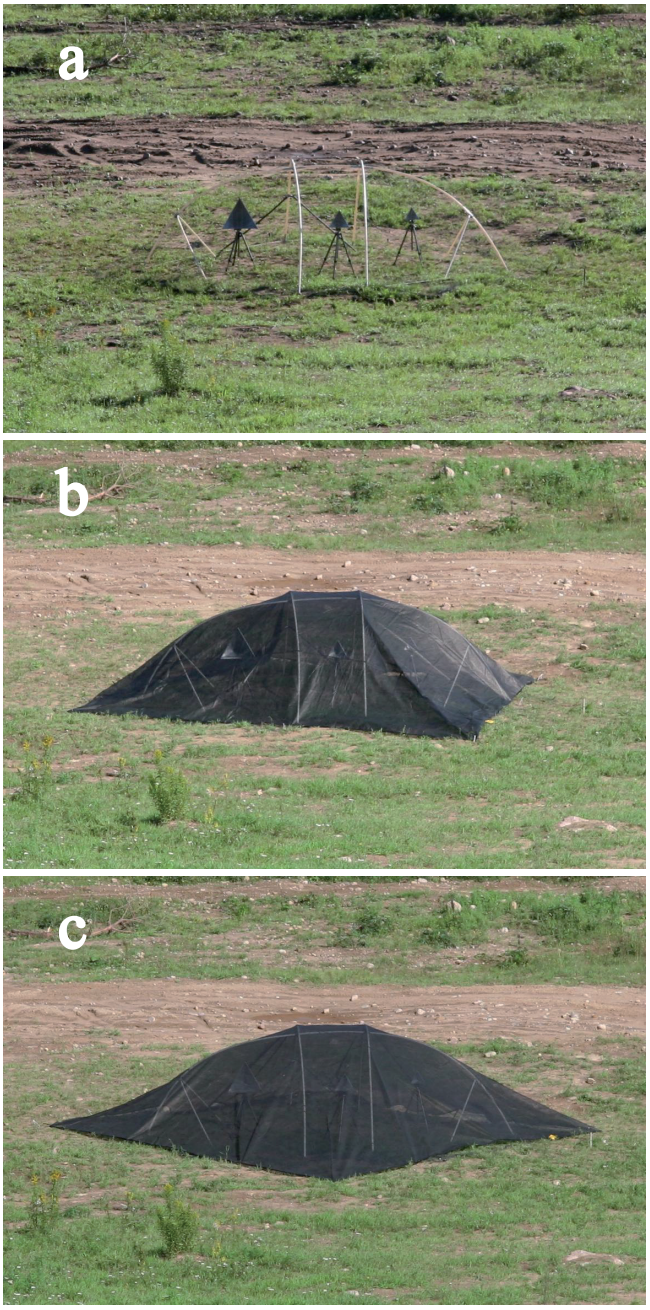

Figure 3. Photographs of a) the three corner reflector reference targets and a low RCS stand for camouflage nets b) corner reflectors covered with a generic low transmission camouflage net and c) corner reflectors covered with a generic high transmission camouflage net.

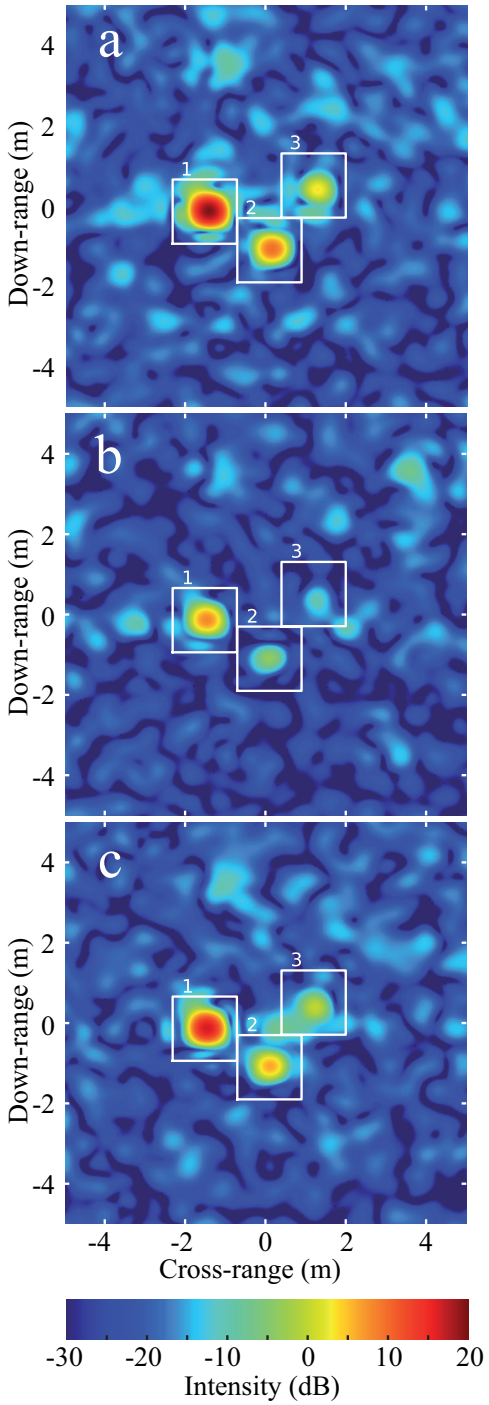

Figure 4. VV polarization SAR images corresponding to the photographs in Figure 3. of a) the three corner reflector reference target b) the low transmission camouflage net and c) the high transmission camouflage net. The RCS for the numbered gates are shown in Table 1. A Hanning filter is used to process the raw data.

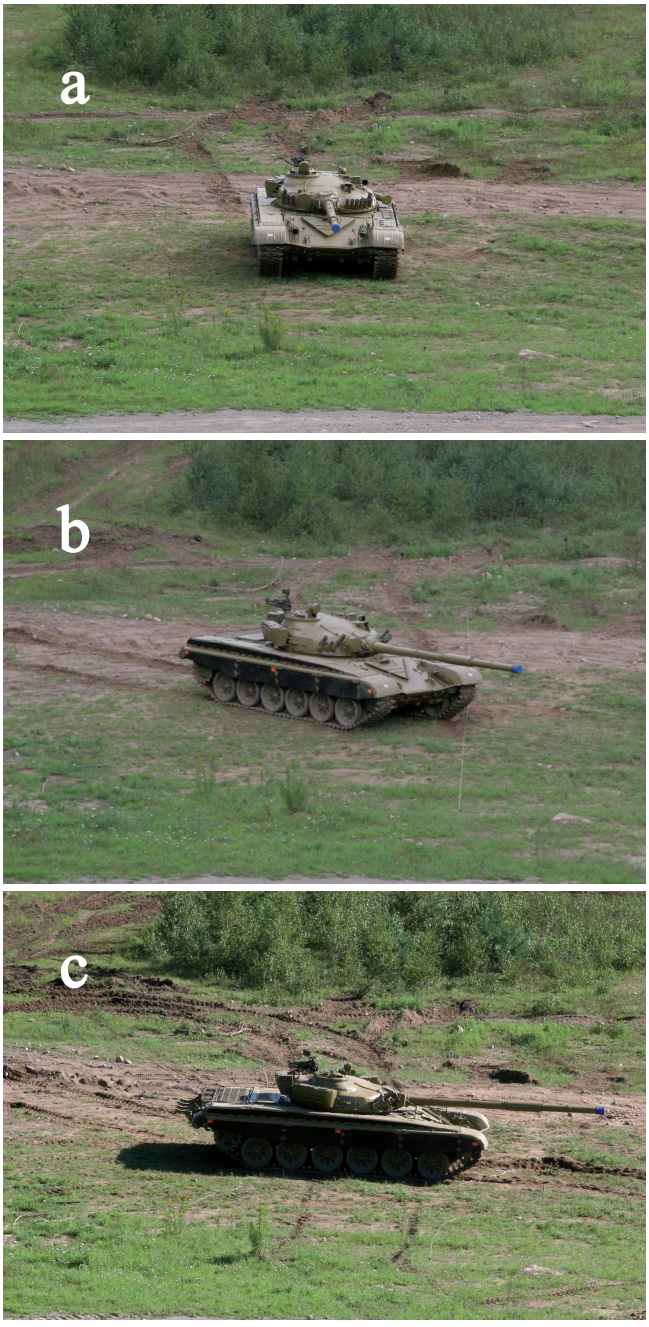

Figure 5. Photographs of the T72 tank at three different angles. The aspect angles are a) 0°, b) 45°c) and 90°.

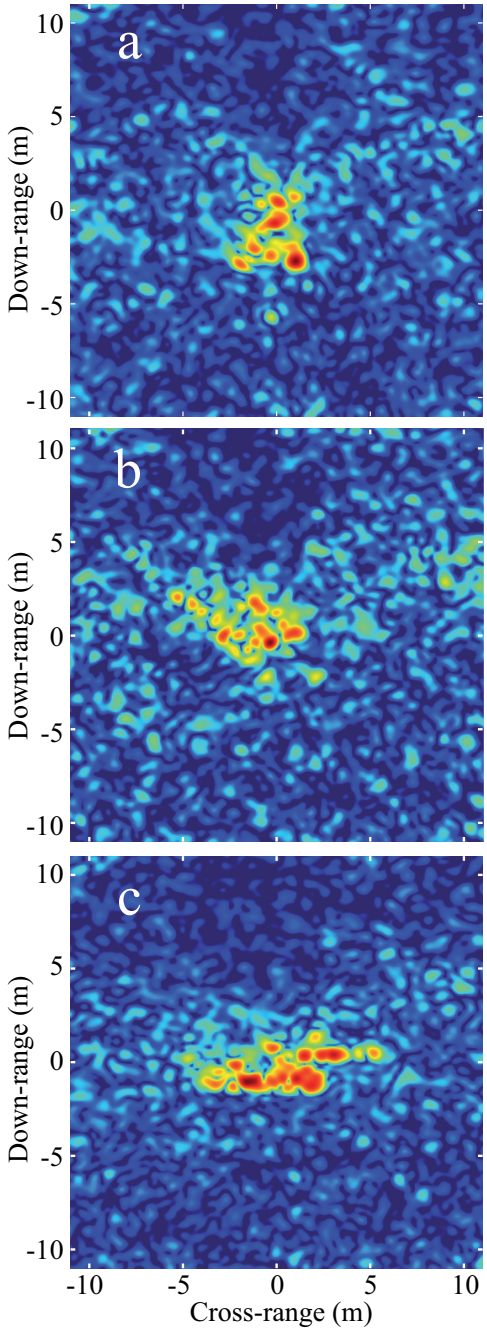

Figure 6. VV polarization SAR images corresponding to the photographs in Figure 5 of the T72 tank at a) 0°, b) 45°and c) 90°. A Hanning filter is used to process the raw data.